

Multi-proxy geoarchaeological study redefines understanding of the paleocoastlines and ancient harbours of Liman Tepe (Iskele, Turkey)

Beverly N. Goodman,¹ Eduard G. Reinhardt,² Hendrik W. Dey,³ Joseph I. Boyce,² Henry P. Schwarcz,² Vasif Sahoğlu,⁴ Hayat Erkanal⁴ and Michal Artzy⁵

¹Interuniversity Institute for Marine Sciences-Eilat, Coral Beach 88000, Israel; ²McMaster University, School of Geography and Earth Sciences, Hamilton, ON L8S4K1, Canada; ³American Academy in Rome, Via Angelo Masina 5, Rome 00153, Italy; ⁴Department of Archaeology, Ankara University, Sıhhiye-Ankara TR-06100, Turkey; ⁵Department of Maritime Civilizations/Recanati, University of Haifa, Institute of Maritime Studies, Haifa 31905, Israel

ABSTRACT

Determining the position of Liman Tepe's (ancient 'Clazomenae') archaeological features relative to the coastline is important for understanding their intended function and reconstructing the character of Aegean maritime activities and sea-based trade. Previous attempts at reconstructing harbour locations at Liman Tepe relied on extrapolating paleoenvironments based on modern surface topography. In light of this, samples from a sediment coring survey and terrestrial and underwater archaeological excavations were analysed using multi-proxy geoarchaeological methods to determine paleoenvironmental facies. Micropaleontological (foraminifera), sedimentological (grain-size analysis) and geochemical ($\delta^{13}\text{C}/\delta^{18}\text{O}$) analyses resulted in the reconstruction of

the coastal paleogeomorphology, including the presence and absence of ancient harbouring areas. Neither of the previous coastal reconstructions was supported by the new results. Instead, two separate harbouring areas were recognized, one coincident with the Early Bronze Age (4800–3900 years BP) and a second during the archaic and classical periods (c. 2800–2400 years BP). These results emphasize the necessity for multi-proxy geoarchaeological studies when approaching coastal archaeological sites as a means to reconstruct paleocoastal geomorphology and understand ancient maritime development better.

Terra Nova, 21, 97–104, 2009

Introduction

Previous paleogeographical reconstructions of the archaeological site Liman Tepe (Fig. 1) have been, like many coastal archaeological studies, limited to using topography and archaeological data from surface surveys to extrapolate previous coastline positions (see Ersoy, 1993). Beginning in 1999, underwater excavations of a submerged feature adjacent to the coastline brought previous coastal reconstructions into question and necessitated approaching the issue using extensive multi-core subsurface data analysed with multi-proxy environmental proxies. Paleogeographical coastal studies along archaeologically-rich coastlines are central to reconstructing ancient coastlines, understanding ancient maritime activities and estimating future coastal change (Reinhardt and Raban, 1999; Marriner and Morhange, 2007). At

present, the accuracy of such studies is even more important given an exponentially increasing human population, expected sea-level rise as a result of global warming and projected coastal development.

Lesser known, but no less significant than its contemporaneous neighbor Troy to the north, Liman Tepe played a major role in the development of trade linking the Mediterranean and Aegean to the Asian continent during the Chalcolithic (5500–4800 years BP) and Early Bronze Age (EBA 4800–3900 years BP) (Erkanal and Günel, 1996; Erkanal and Artzy, 2002; Şahoğlu, 2002, 2005). Subsequently, Liman Tepe became a member of the Ionian League, a confederacy formed as early as 800 BC, which played a significant role in the power struggles between Persians and Greeks, most famously during the Ionian Revolts (499–494 BC). These battles were the first phase of conflicts within the 'Greco-Persian Wars' (499–444 BC, Herodotus). A century later, a causeway built from the island to the mainland is credited to Alexander the Great (335 BC, Heisserer, 1980).

Researchers from the Izmir Region Excavations and Research Project provisionally identified a submerged feature as the remains of an EBA harbour structure on the basis of similarities in construction materials and proximity to the terrestrial EBA archaeological site (Fig. 1). Another reconstruction based on the distribution of surface and near-surface archaeological remains indicated a large bay during the archaic period (c. 2800 years BP, Ersoy, 1993; Fig. 1). Based on these observations, underwater archaeological excavations (University of Haifa and Ankara University) and a multi-proxy geoarchaeological study (McMaster University) were initiated to determine the origin and age of the submerged feature and to reconstruct more broadly the coastal landscape of Liman Tepe.

Methods

Terrestrial cores (0.5 to 5-m length) were collected with an Eijkelkamp percussion corer system. The underwater samples were collected by grab

Correspondence: Beverly N. Goodman, Interuniversity Institute for Marine Sciences-Eilat, Coral Beach 88000, Israel. e-mail: goodman@research.haifa.ac.il

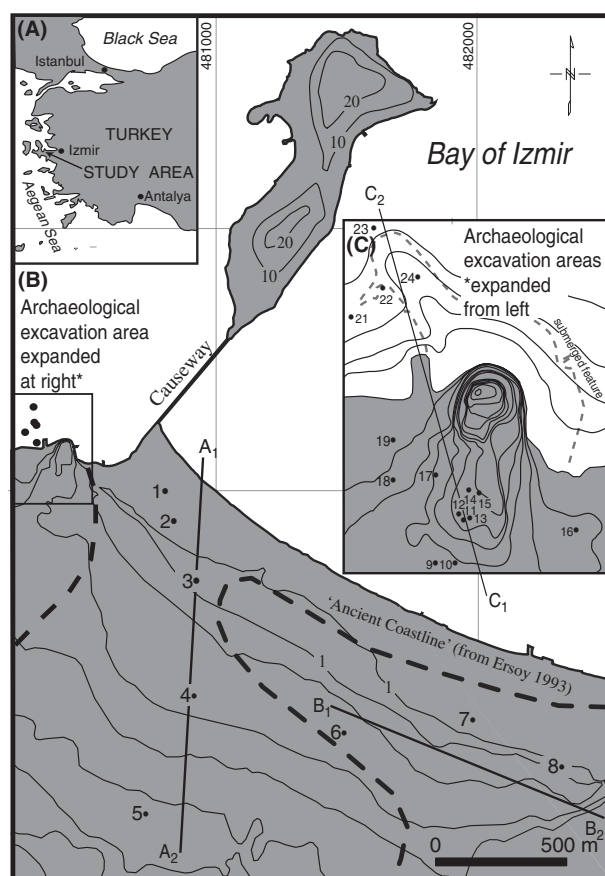


Fig. 1 Location of Liman Tepe. (A) Map of western Turkey. Study area is located west of Izmir. (B) Local map of study area with previous landscape reconstruction represented with a thick dashed line. (C) Expansion of archaeological excavation portion of the study site highlighted in map B. Transsects A, B and C are indicated and coring locations are indicated with circles and associated core number. Unlabelled contours = 1 m.

sampling the exposed baulk sections within the archaeological trenches (see Dean *et al.*, 1994 for methods) and by collecting cores (2 to 4.5-m length) from the seabed.

The relative horizontal positions and chronological constraints of environmental facies (defined based on multiproxy analysis) were then compared to produce a model of coastal change. Previously analysed data (Goodman *et al.*, 2008) from outside the archaeological site (cores 1–8) were combined with data in this study (see Tables 1 and 2) to determine whether previously established facies categories were conserved and to consider those facies in the context of related anthropogenic activities. Micropaleontological analysis and environmental interpretations followed methods described in Scott

et al. (2001) and Scott and Medioli (1986). Species of microfossils with a wide range of environmental tolerances were isolated to determine $\delta^{18}\text{O}$ and $\delta^{13}\text{C}$ values in the near-coastal environment (see Reinhardt *et al.*, 2001 and references therein). Overall averages for each biofacies were used to determine the presence of general environmental facies trends. An aliquot of each sample was subsampled and processed to determine particle-size distribution (methods Goodman *et al.*, 2008), which was then evaluated across cores. Comparative samples from the modern terrestrial surface and uppershoreface seafloor were analysed to provide a basis for defining environmental facies. Dated samples with known position relative to sea-level were plotted in comparison with previously

established sea-level curves (see Figs 2 and 3).

Results

The paleogeography is reconstructed using the relative positions of environmental facies based on core summaries and sea level markers (Figs 2 and 3). Environmental facies include terrestrial, supratidal, wetland, foreshore, lagoon, upper shoreface, and harbour (see Tables 1 and 2).

The terrestrial biofacies are defined by an absence of or low foraminifera abundance (less than 2 specimens per cm^3 , broken or eroded when present), silt-range grain-size average values and, in some cases, continuity with the modern surface (see Figs 2 and 3, Tables 1 and 2). The isotope value averages were $\delta^{18}\text{O} = -1.2\text{‰}$ (depleted by -2‰ relative to local seawater) and $\delta^{13}\text{C} = -2.4\text{‰}$ (local marine values $c.1.5\text{‰}$).

The foreshore facies is distinguished by low-abundance (average of eight specimens per cm^3) microfossils and therefore is distinguished from terrestrial primarily by grain-size averages, increased presence of marine fauna (e.g. marine gastropods, shell fragments) and position downcore. Grain-size averages range from fine to coarse sand and isotope value averages are $\delta^{18}\text{O} = -0.7\text{‰}$ and $\delta^{13}\text{C} = -2.4\text{‰}$.

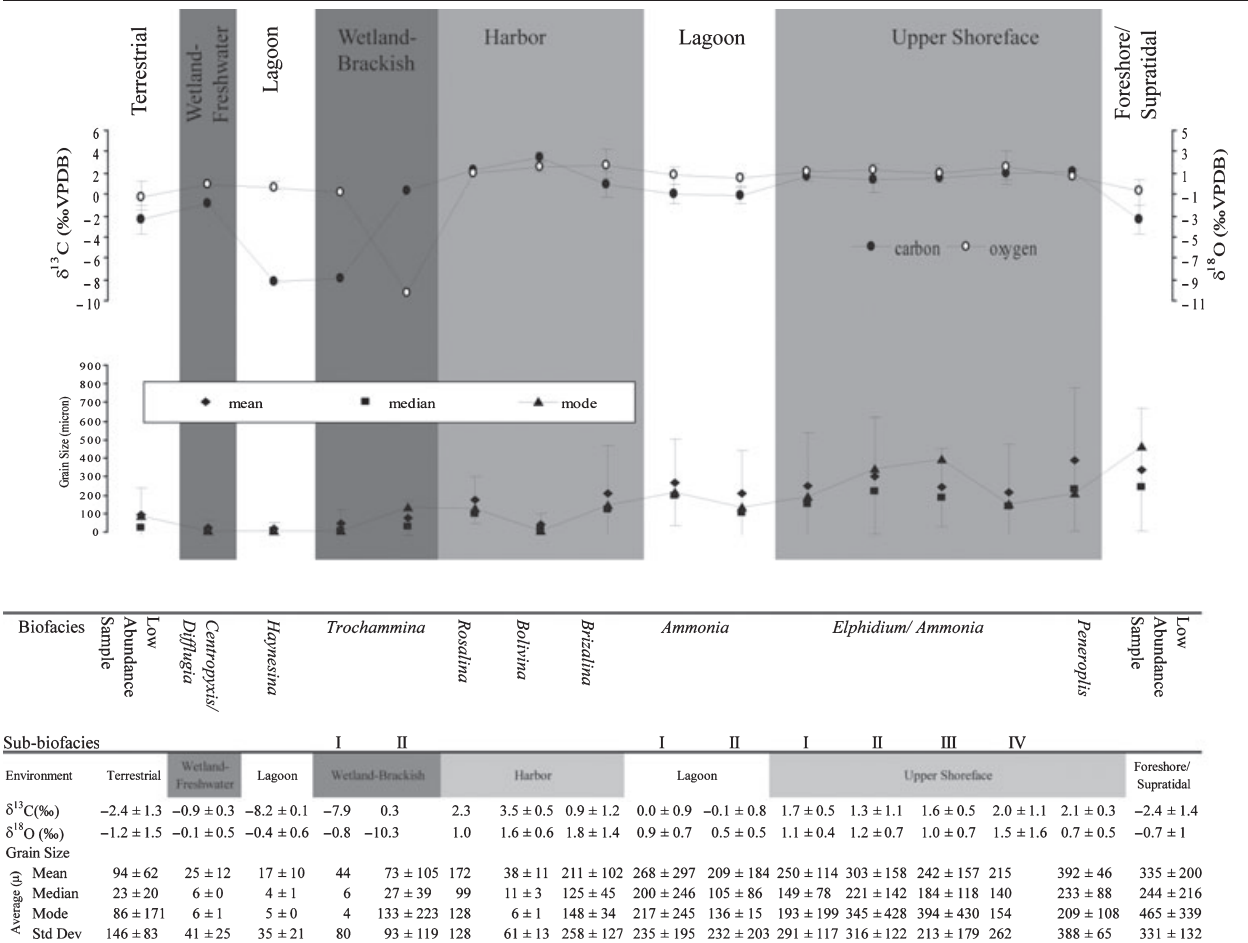
The lagoon facies is defined by *Haynesina*, *Ammonia* I and II biofacies groups. *Ammonia* I is distinguished by the dominance of *A. parkinsoniana* 'tepida' (71%) and *Trochammina* spp. The *Ammonia* II biofacies is distinguished by 19.3% *A. parkinsoniana* 'tepida', and similar abundances of *Rosalina bradyi*, *Eponides* sp A, *Elphidium macellum*, *Asterigina mamilla*, and *Cibicides refulgens*. Grain-size averages range from fine to coarse sands with high standard deviation values. The *Ammonia* I isotope values are $\delta^{18}\text{O} = 0.0\text{‰}$ and $\delta^{13}\text{C} = 0.9\text{‰}$. *Ammonia* II values are $\delta^{18}\text{O} = -0.1\text{‰}$ and $\delta^{13}\text{C} = 0.5\text{‰}$. The $\delta^{13}\text{C}$ values of *Ammonia* I and *Ammonia* II are within marine values and the $\delta^{18}\text{O}$ values are about 1‰ depleted relative to seawater values.

A majority of samples (38 of 67) with high foraminiferal abundance clustered into the upper shoreface facies (marine). The five biofacies in this group include *Elphidium/Ammonia*

Table 1 Biofacies as determined by Ward's method clustering of normalized distributions of foraminifera. Table presents all foraminifera species in which abundance equals a minimum of 1% in a minimum of one biofacies after accounting for error. All diversity indexes determined using PAST software (Hammer *et al.*, 2001).

Biotypes	Trochammina										Ammonia										Elphidium /Ammonia										Peneroplis																		
	Centropyxis /Diffugia					Rosalina					Bolivina					Brizalina					Haynesina					I						II					III					IV							
	Wetland-Freshwater					Wetland-Brackish					Harbour					Lagoon																																	
Environmental	Interpretation	Total no. of Samples					2	1σ	3	1σ	1	1σ	3	1σ	8	1σ	3	1σ	6	1σ	3	1σ	16	1σ	9	1σ	8	1σ	1	1σ	4	1σ																	
	No. of individuals per cc	139 ± 47	16 ± –	28 ± 10	496 ± –	31 ± 1	325 ± 236	83 ± 10	286 ± 166	61 ± 28	756 ± 719	222 ± 342	41 ± 37	87 ± –	391 ± 155																																		
	Number of Taxa in sample	7 ± 1	3 ± 1	3 ± 1	38 ± –	30 ± 37	35 ± 8	7 ± 4	9 ± 3	37 ± 5	42 ± 6	41 ± 8	27 ± 4	34 ± –	41 ± –																																		
	Shannon H Diversity	0.75 ± 0.2	2.11 ± –	0.23 ± 0.2	2.20 ± –	2.79 ± 1.0	3.07 ± 0.2	1.7 ± 0.2	0.91 ± 0.3	3.04 ± 0.2	3.40 ± 0.2	3.29 ± 0.3	2.91 ± 0.2	1.94 ± –	3.31 ± –																																		
	Abdiodontrix rhomboidalis	–	1.2 ± –	–	0.3 ± –	2.2 ± 0.5	3.1 ± 2.4	–	0.1 ± 0.2	3.3 ± 4.4	2.4 ± 2.0	0.7 ± 1.0	–	0.4 ± –	0.7 ± 0.8																																		
	Ammonia parkinsoniana	0.8 ± 1.1	–	–	2.3 ± –	0.5 ± 0.5	2.5 ± 1.5	1.1 ± 0.8	6.5 ± 8.9	3.2 ± 4.3	1.4 ± 1.7	8.3 ± 4.3	6.7 ± 4.3	56.5 ± –	1.9 ± 2.8																																		
	Ammonia park. 'tepidia'	1.1 ± 1.5	16.0 ± –	0.2 ± 0.3	–	0.1 ± 0.2	0.8 ± 1.0	0.4 ± 0.4	71.4 ± 111.9	19.3 ± 4.5	2.6 ± 3.2	2.5 ± 2.5	0.8 ± 2.1	–	2.3 ± 2.2																																		
	Ammonia sp. A	–	–	–	–	–	–	–	–	–	–	0.2 ± 0.4	8.2 ± 5.2	–	0.5 ± 0.5																																		
	Asterigerinata namilla	–	–	–	3.0 ± –	0.1 ± 0.2	1.6 ± 1.4	–	–	4.0 ± 2.7	1.3 ± 1.1	1.6 ± 1.4	2.2 ± 1.9	1.6 ± –	0.5 ± 0.3																																		
	Bolivina pseudoplicata	–	1.2 ± –	0.3 ± 0.5	4.4 ± –	23.2 ± 4.3	6.1 ± 5.2	–	–	1.7 ± 0.8	2.1 ± 1.9	1.9 ± 1.3	0.6 ± 1.1	0.1 ± –	2.6 ± 2.1																																		
	Brizalina striatula	–	0.6 ± –	–	1.2 ± –	3.2 ± 0.8	8.3 ± 2.4	–	0.2 ± 0.3	3.6 ± 3.1	1.7 ± 1.7	2.1 ± 2.2	1.2 ± 2.6	3.9 ± –	1.1 ± 1.6																																		
	Centropyxis aculeate	42.7 ± 11.4	2.5 ± –	–	–	–	–	–	–	–	–	–	–	–	–																																		
	Centropyxis onstricia-silica	27.3 ± 11.2	–	–	–	–	0.3 ± 0.7	–	–	–	–	–	–	–	–																																		
	Cibicides refulgens	–	–	–	3.0 ± –	3.1 ± 1.8	4.3 ± 2.1	–	–	4.0 ± 2.5	3.5 ± 1.9	3.3 ± 2.2	2.7 ± 2.7	0.1 ± –	1.6 ± 0.4																																		
	Cornuspira foliacea	–	–	–	0.1 ± –	4.1 ± 2.2	0.2 ± 0.3	–	–	0.1 ± 0.1	0.5 ± 0.8	0.1 ± 0.2	0.2 ± 0.7	–	0.8 ± 0.8																																		
	Diffugia oblonga	25.5 ± 3.0	–	–	–	–	–	–	–	–	–	–	–	–	–																																		
	Elphidium advenum	0.2 ± 0.2	–	–	0.3 ± –	1.2 ± 0.6	2.6 ± 1.4	–	–	2.2 ± 1.6	3.2 ± 1.5	4.4 ± 1.7	8.7 ± 7.4	3.8 ± –	4.7 ± 0.7																																		
	Elphidium jenseni	–	–	0.2 ± 0.4	3.5 ± –	1.6 ± 1.4	3.2 ± 2.8	–	0.6 ± 1.4	2.7 ± 2.3	2.5 ± 1.4	3.0 ± 2.4	0.8 ± 2.2	4.5 ± –	1.6 ± 1.7																																		
	Elphidium macellum	0.2 ± 0.2	0.6 ± –	–	3.4 ± –	0.8 ± 1.5	2.3 ± 1.7	–	0.1 ± 0.1	4.8 ± 2.5	3.1 ± 2.7	7.0 ± 1.9	5.2 ± 3.6	5.7 ± –	4.2 ± 1.1																																		
	Elphidium translucens	–	–	–	3.0 ± –	–	3.5 ± 4.2	–	–	2.4 ± 3.6	1.8 ± 1.0	2.3 ± 1.4	1.3 ± 1.0	2.0 ± –	0.9 ± 0.9																																		
	Eponides sp. A	–	3.1 ± –	–	1.7 ± –	2.7 ± 2.4	3.5 ± 3.5	–	–	6.2 ± 1.2	4.7 ± 1.9	4.5 ± 2.6	3.7 ± 3.5	1.2 ± –	2.6 ± 2.3																																		
	Haynesina depressula	–	–	–	–	–	6.0 ± 6.0	9.6 ± 6.1	1.5 ± 3.5	4.1 ± 3.2	3.9 ± 2.1	4.2 ± 4.0	1.1 ± 2.1	4.3 ± –	1.5 ± 1.4																																		
	Haynesina sp. D	–	–	–	–	–	–	78.0 ± 9.9	–	–	–	–	–	–	–																																		
	Miliolinella sp. B	–	0.6 ± –	–	2.1 ± –	7.0 ± 3.5	2.7 ± 2.0	–	–	0.6 ± 0.6	4.4 ± 2.7	1.2 ± 1.2	–	0.3 ± –	2.4 ± 1.9																																		
	Peneroplis pertusus	–	–	–	0.1 ± –	0.2 ± 0.4	0.1 ± 0.3	–	–	–	0.3 ± 0.6	0.3 ± 0.7	1.3 ± 1.9	–	11.1 ± 5.6																																		
	Pseudotriloculina cuneata	–	3.1 ± –	–	0.1 ± –	3.7 ± 1.0	1.0 ± 1.5	–	0.2 ± 0.4	2.1 ± 0.9	4.5 ± 1.6	2.7 ± 1.8	0.3 ± 0.6	0.7 ± –	2.3 ± 3.5																																		
	Pseudotriloculina laevigata	–	0.6 ± –	–	1.8 ± –	5.6 ± 1.1	0.3 ± 0.4	–	–	0.7 ± 0.8	1.4 ± 1.4	0.5 ± 0.6	0.1 ± 0.2	0.1 ± –	1.3 ± 2.0																																		
	Quinqueloculina patagonica	–	1.8 ± –	–	1.7 ± –	7.8 ± 3.5	2.2 ± 2.4	–	–	1.2 ± 2.1	2.3 ± 1.1	2.1 ± 1.9	0.6 ± 0.9	0.1 ± –	1.1 ± 0.8																																		
	Rosalina bradyi	–	0.6 ± –	0.1 ± 0.2	50.7 ± –	1.3 ± 0.8	7.1 ± 2.9	–	–	4.9 ± 0.7	5.6 ± 3.4	7.2 ± 6.4	3.1 ± 2.6	–	2.4 ± 1.3																																		
	Rosalina floridensis	–	–	–	2.8 ± –	3.6 ± 1.5	3.7 ± 4.3	–	–	–	2.5 ± 3.0	0.7 ± 0.6	0.6 ± 0.9	–	0.7 ± 0.8																																		
	Trilobulina subgranosum	–	–	–	0.5 ± –	–	–	–	4.1 ± 5.7	–	–	–	0.4 ± 0.8	–	–																																		
	Trochammina inflata	–	21.5 ± –	5.7 ± 9.9	–	0.6 ± 0.3	4.5 ± 6.2	–	2.1 ± 4.1	2.1 ± 1.2	0.3 ± 0.7	0.5 ± 0.8	–	0.4 ± –	0.5 ± 0.9																																		
	Trochammina macraters	–	15.3 ± –	–	–	–	0.2 ± 0.4	–	2.8 ± 4.9	0.9 ± 0.9	0.4 ± 0.9	0.7 ± 1.6	–	–	–																																		
	Trochammina sp. A	0.8 1.1	23.3 ± –	93.1 ± 9.4	–	–	0.1 ± 0.3	–	–	–	–	–	–	–	–																																		
	Total Represented %	98	92	100	86	73	70	89	90	74	56	62	50	86	49																																		

Table 2 Average isotope and grain size values in environmental facies. Standard deviation of values is one sigma. Values with no standard deviation had only one sample in the biofacies. Low abundance samples have less than foraminifera per cm³.



I-IV and *Peneroplis*. *Elphidium/Ammonia* clusters I-IV consist of high-diversity samples containing shoreface-preferring taxon. The *Elphidium/Ammonia* biofacies have a greater than 10% presence of major abundance of *Elphidium* (*E. advenum*, *E. jenseni*, *E. macellum*, *E. translucens*) and the presence of *A. parkinsoniana*. The *Peneroplis* cluster is dominated by *P. pertusus* (11%), *Elphidium advenum* (4.7%), and *E. macellum* (4.2%). All upper shoreface facies grain-size averages range from fine to coarse sands with large standard deviations, indicating poor sorting. *Elphidium/Ammonia* upper shore facies isotopic averages range from δ¹⁸O = 1.0 to 1.5‰ and δ¹³C = 1.3 to 2.0‰. *Peneroplis* upper shoreface isotope values are δ¹⁸O = 1.5‰ and average δ¹³C = 2.1‰. All of the average values are marine or near-marine.

There are three biofacies groups in the harbour facies, which reflect the eutrophic artificial harbour environment ('*Brizalina*' and '*Bolivina*' biofacies) and post-harbour ('*Rosalina*' biofacies). Average grain-size values are fine sand and average isotopic values are δ¹⁸O = 1.8‰ and δ¹³C = 0.9‰. The post-harbour facies is dominated by *Rosalina bradyi* (50%), fine sand-size sediment and average isotopic values of δ¹⁸O = 1.0‰ and δ¹³C = 2.3‰. Samples collected from the clay-rich matrix of the primarily framework-supported rubble deposit in Area 24, an archaeological trench in the submerged portion of the site (see Fig. 1 for location), clustered independently into a *Bolivina pseudoplicata*-dominated biofacies. The abundance of foraminifera in these samples is lower than in the normal marine facies (*c.*30 specimens

per cm³ vs. 300 specimens per cm³), grain-size values are finer and isotope averages are within marine values (δ¹⁸O = 1.6‰ and δ¹³C = 3.5‰).

Discussion

The results provide a view of the local sea-level trends and related environmental change. The sea-level markers were in agreement with previous regional models (Peltier, 1994; Lambeck, 1995; Lambeck and Bard, 2000; Lambeck *et al.*, 2004; see Figs 2 and 3). The environmental facies relationships between the cores described herein show that the coastal environment consisted of marine transgression from an estimated 9000 to 6000 years BP, followed by sea-level rise deceleration (see Figs 2 and 3A). The deceleration resulted in a positive coastal sediment budget, which, when

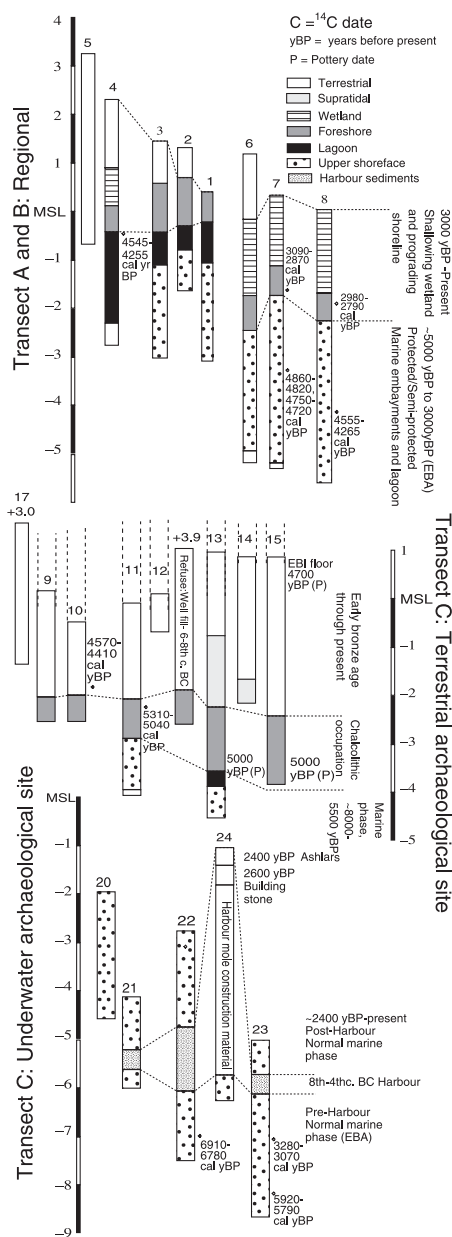


Fig. 2 Cores with facies designations, radiocarbon dates and dated materials relative to mean sea level (msl). Cores 16, 18, and 19 were short cores (less than 1.5-m length) characterized only by terrestrial facies, were consistent with the surrounding stratigraphy and were therefore excluded due to redundancy. Transect positions are shown in Fig. 1.

transported by the long-shore currents, created a consecutive series of sandbars that ultimately lead to beach barrier development. These sandbars contributed to the creation of near-shore lagoons and a tombolo formation that provided quiet anchorage for seafaring vessels during the EBA (4800–3900 years BP; see Fig. 3B,E). That same process of long-shore transport eventually isolated the

lagoons from the sea (see Fig. 3C), ending the area's usefulness for harbouring activities. Between the final closure of the lagoon (c. 3000 years BP) and the construction of the quay structure at c. 2800 years BP, there is no evidence of a harbour, natural or otherwise, in the landscape. At c. 2800 years BP, artificial harbouring structures were constructed (Fig. 3C). Eventually, gradual sea-level rise and

erosion of the structure led to its present position 1 m below sea-level (see Fig. 3D). The construction of a causeway probably accelerated the process of coastal progradation towards the east (Goodman *et al.*, 2008).

The information from this study helps provide the means to interpret between coastal changes and associated archaeological phases, most notably with regard to the time of appearance and disappearance of harbouring areas. During the EBA, large lagoon areas east of the site provided the necessary conditions for anchorage and/or beaching of boats (see Figs 3B,E), which supplied sea-based trade goods found at the site (Şahoğlu, 2005). If artificial harbouring structures existed in that period, they would most likely be located on the margins of those lagoons. A second harbouring area would have existed in the protected waters leeward of the headland (Figs 3B,E). These findings are in agreement with current theories regarding early Aegean sea-based maritime trade, which state that shipping during the EBA depended on the opportunistic use of natural harbours such as embayments and lagoons (Raban, 1985; Stanley and Warne, 1994; Wachsmann, 1998).

At approximately 3000 years BP, the brackish-marine lagoon areas east of the site became freshwater, indicating final closure and isolation of the area from marine influence (see Fig. 3 and Goodman *et al.*, 2008). Culturally, this event coincides with the transition between the Late Bronze Age and Early Iron Age, a period that is relatively poor in cultural materials relative to the phases, which preceded and followed it. As the earliest traces of harbour facilities elsewhere at the site begin c. 2800 years BP, there is no evidence for a functional harbour for some two centuries following the closure of the brackish-marine lagoon, an absence which perhaps reflects a real – albeit temporary – decline in maritime trade and communication in the area.

The submerged feature abutting the archaeological site constitutes clear evidence for harbour activity during the archaic and classical periods (c. 2800 years BP to 2400 years BP). Core 24 represents the central spine of the structure, the rubble foundation of which was laid directly on the seafloor

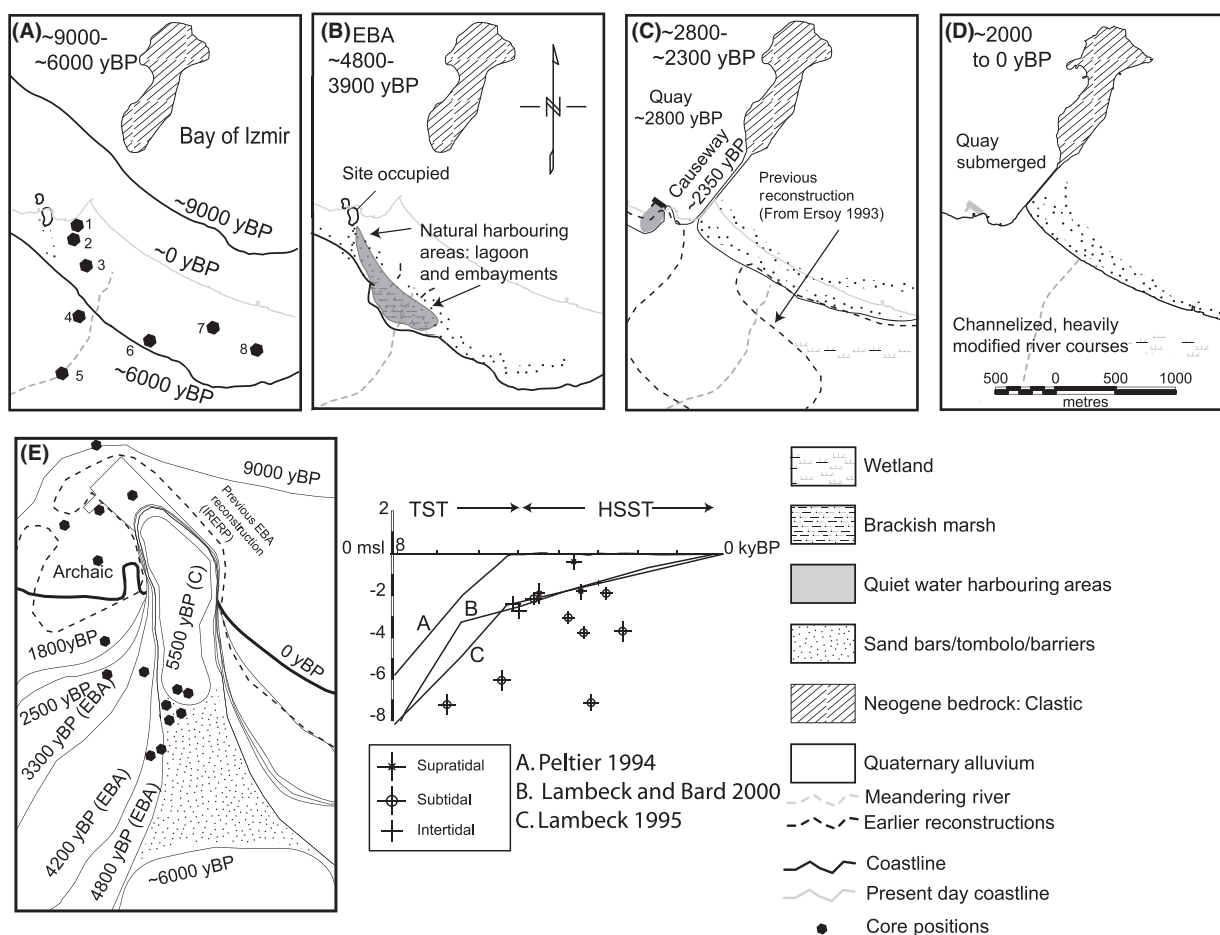


Fig. 3 Top plan of paleogeography and sea level curve. (A) Peltier, 1994; (B) Lambeck and Bard, 2000; (C) Lambeck, 1995.

(see Fig. 1C and 2 transect C). It remains to be established whether the entire length of the main body of the submerged feature, or merely a portion, is anthropogenic. All areas excavated reveal an artificial feature, although there is the possibility that bedrock knolls, smaller versions of the distinctive headland nearby, may have provided framework. The further possibility that the harbour included a second 'arm' farther to the west of the site also merits future exploration. In any case, the sedimentological, micro-paleontological and geochemical data indicate the presence of a typical normal marine environment prior to the construction of the feature (pre-2800 years BP), followed by a more constricted, lower energy environment characteristic of sheltered harbours (c. 2800–2400 years BP) and finally, a return to normal marine conditions after the abandonment and/or partial destruction of the harbouring feature

(c. 2400 years BP), when it no longer sufficed to block wave energy. Substantial quantities of archaeological material consonant with a harbour environment (including a recently-discovered wooden anchor, Artzy *et al.*, 2007) discovered in the vicinity of the quay confirm the identification of the port and provide good indicators for its dating.

Coastal geomorphology is also dependent on climate. Increased humidity and precipitation can result in increased terrestrial erosion, higher rates of sediment input and enriched vegetation (Aksu *et al.*, 1995). Paleoclimate studies conducted nearest to Liman Tepe describe higher humidity and higher temperatures from 4500 to 2600 years BP (Baruch, 1994), which includes the EBA through Archaic Period. The combined effects of humidity-driven increased sediment input and decreased erosion effects from deceleration of sea-level rise

correspond well with the eventual closure of the EBA lagoonal areas.

Conclusion

Two conclusions emerge which stand in contrast to previous coastal reconstructions of the Liman Tepe site. First, the submerged feature was not associated with the EBA phase, but rather with a harbour installation in use from approximately 2800 to 2400 years BP. Second, while there was a large bay east of the site, it existed during the Bronze Age only, but not during the Archaic and/or Classical Periods as previously thought (see maps in Ersoy, 1993 and Bakır *et al.*, 2000). The paleogeographical reconstruction of Liman Tepe thus supports the theory that the coastal landscape of the EBA featured a relative abundance of natural harbouring locations, such that existing levels of shipping could be accommodated without re-

course to extensive construction of artificial harbours. The intervening timespan (from c. 3000 years BP to c. 2800 years BP) between the silting of the older, natural harbour and the construction of the new harbour to the west, during which neither natural nor artificial harbouring areas can be shown to have existed, coincides with a period of reduced quantities of cultural materials (including overseas imports) at the adjacent settlement.

Previous geoarchaeological studies near Liman Tepe have addressed sites located at the mouths of large rivers, where coastal sites are now located far inland (e.g. Ephesus, Brückner, 1997; and Troy, Kraft *et al.*, 2003). This study, in contrast, illustrates the major coastal changes that can occur in less dynamic environments, even without a major alluvial point source. More broadly, it exemplifies the utility of multi-proxy geoarchaeological method in establishing the relationship between natural coastal processes and the human occupants of a littoral site over the course of several millennia. The study of ancient harbouring facilities is essential to understanding human impacts on the coastal environment, influence of landscape and resources on ancient site selection, sea-level change and effects of coastal change on human settlements (e.g. Flemming and Webb, 1986; Kayan, 1988; Fleming *et al.*, 1998; Morhange *et al.*, 2000, 2001; Rothaus *et al.*, 2004; Marriner *et al.*, 2006; Reinhardt *et al.*, 2006; Marriner and Morhange, 2007).

Acknowledgements

This research was supported by Archaeological Institute of America, Geochron Laboratories, Women's Diving Hall Of Fame, Geological Society of America, Hatter Foundation, Turkish Ministry of Culture, Ankara University Research Fund Project No: 2006-0901024, TUBITAK Project No: 108K263, INSTAP, Urla Municipality and an anonymous donor. Many thanks are to A.Yurman, S. Breistein, G. Votruba, A. Haggi, M. Knyff, D. Tchernov, B. Chapman, and the reviewers whose criticisms and detailed corrections greatly improved the manuscript.

References

Aksu, A.E., Yaşar, D., Mudie, P.J. and Gillespie, H., 1995. Late glacial-Holocene paleoclimatic and paleoceanographic evolution of the Aegean Sea: micropaleontological and stable isotopic evidence. *Mar. Micropaleontol.*, **25**, 1–28.

- Artzy, M., Goodman, B., Haggi, A., Votruba, G. and Soloman, Y., 2007. *Liman Tepe Underwater Archaeological Report*. RIMS, Haifa.
- Bakır, G., Ersoy, Y., Fazlioglu, I., Aytaclar, N., Cevizoglu, H., Hurmuzlu, B. and Sezgin, Y., 2000. 1999 *Klazomenai Kazisi. Paper presented at the Kazi Sonuclari Toplantisi*, Izmir.
- Baruch, U., 1994. The Late Quaternary pollen record of the Near East. In: (O. Bar-Yosef and R. Kra, eds). *Late Quaternary Chronology and Paleoclimates of the Eastern Mediterranean*, Peabody Museum of Archaeology and Ethnology, Harvard University, Cambridge, MA, pp. 103–120.
- Brückner, H., 1997. Coastal Changes in Western Turkey; Rapid Delta Progradation in Historical Times. *Bull. Inst. Océanogr.*, **18** (Special Number 18), 63–74.
- Dean, M., Ferrari, B., Oxley, I., Redknap, M. and Watson, K., 1994. *Archaeology Underwater: NAS Guide to Principles and Practice*. Archetype Books, London, 332 p.
- Erkanal, H. and Artzy, M., 2002. 2000 Yılı Liman Tepe Kazısı çalışmaları. *Kazi Sonuclari Toplantisi*, **XXIII**, 375–383. (in Turkish).
- Erkanal, H. and Günel, S., 1996. 1994 Yılı Liman Tepe Kazisi XVI. *Kazi Sonuclari Toplantisi*. Ministry of Culture, Ankara, 305–327.
- Ersoy, Y., 1993. *Clazomenae: The Archaic settlement*. PhD Thesis, Bryn Mawr College, 320 p.
- Fleming, K., Johnston, P., Zwart, D., Yokohama, Y., Lambeck, K. and Chappell, J., 1998. Refining the eustatic sea level curve since the Last Glacial Maximum using far and intermediate field sites. *Earth Planet. Sci. Lett.*, **163**, 327–342.
- Flemming, N.C. and Webb, C.O., 1986. Tectonic and eustatic coastal changes during the last 10000 years derived from archaeological data. *J. Geom. N.F.*, **62**, 1–29.
- Goodman, B., Reinhardt, E., Dey, H., Boyce, J., Schwarcz, H., Şahoğlu, V., Erkanal, H. and Artzy, M., 2008. Evidence for Holocene Marine Transgression and Shoreline Progradation due to Barrier Development in Iskele, Bay of Izmir, Turkey. *J. Coastal Res.*, **24**, 1269–1280.
- Hammer, Ø., Harper, D.A.T. and Ryan, P.D., 2001. PAST: Paleontological Statistics Software Package for Education and Data Analysis. *Palaeontol. Electronica*, **4**, http://palaeo-electronica.org/2001_1/past/issue1_01.htm.
- Heisserer, A.J., 1980. *Alexander the Great and The Greeks*. University of Oklahoma Press, Norman, Oklahoma.
- Kayan, I., 1988. Late Holocene Sea-level changes on the Western Anatolian coast. *Geogr. Climatol. Ecol.*, **68**, 205–218.
- Kraft, J.C., Rapp, G., Kayan, I. and Luce, J.V., 2003. Harbor areas at ancient Troy: Sedimentology and geomorphology complement Homer's *Iliad*. *Geology*, **31**, 163–166.
- Lambeck, K., 1995. Late Pleistocene and Holocene sea-level change in Greece and south-western Turkey: a separation of eustatic, isostatic and tectonic contributions. *Geophys. J. Int.*, **122**, 1022–1044.
- Lambeck, K. and Bard, E., 2000. Sea-level change along the French Mediterranean coast for the past 30 000 years. *Earth Planet. Sci. Lett.*, **175**, 203–222.
- Lambeck, K., Antonioli, F., Purcell, A. and Silenzi, S., 2004. Sea-level change along the Italian Coast in the past 10,000 years. *Quatern. Sci. Rev.*, **23**, 1567–1598.
- Marriner, N. and Morhange, C., 2007. Geoscience of ancient Mediterranean harbors. *Earth Sci. Rev.*, **80**, 137–194.
- Marriner, N., Morhange, C., Doumet-Serhal, C. and Carbonel, P., 2006. Geoscience rediscovers Phoenicia's buried harbors. *Geology*, **34**, 1–4.
- Morhange, C., Goiran, J.P., Bourcier, M., Carbonel, P., Le Campion, J., Rouchy, J.-M. and Yon, M., 2000. Recent Holocene paleo-environmental evolution and coastline changes of Kition, Larnaca, Cyprus, Mediterranean Sea. *Mar. Geol.*, **170**, 205–230.
- Morhange, C., Laborel, J. and Hesnard, A., 2001. Changes of relative sea level during the past 5000 years in the ancient harbor of Marseilles, Southern France. *Geogr. Climatol. Ecol.*, **166**, 319–329.
- Peltier, W.R., 1994. Ice Age Paleotopography. *Science*, **265**, 195–201.
- Raban, A., 1985. The Ancient Harbors of Israel in Biblical Times (From the Neolithic period to the End of the Iron Age). In: *Proceedings of the First International Workshop on Ancient Mediterranean Harbors Caesarea Maritima* (A. Raban, ed.), pp. 11–44. British Archaeological Reports, Oxford.
- Reinhardt, E. and Raban, A., 1999. Destruction of Herod the Great's Harbor at Caesarea Maritima; geoarchaeological evidence. *Geology*, **27**, 811–814.
- Reinhardt, E., Fitton, R. and Schwarcz, H., 2001. Isotopic (Sr, O, C) Indicators of Salinity and Taphonomy in a Marginal Marine System. *J. Foramin. Res.*, **33**, 262–272.
- Reinhardt, E., Goodman, B., Boyce, J., Lopez, G., van Hengstum, P., Rink, W.J., Mart, Y. and Raban, A., 2006. The

- Tsunami of 13 December A.D. 115 and the Destruction of Herod the Great's Harbor at Caesarea Maritima, Israel. *Geology*, **34**, 1061–1064.
- Rothaus, R., Reinhardt, E. and Nolan, J., 2004. Regional Considerations of Coastline Change, Tsunami Damage and Recovery along the Southern Coast of the Bay of Izmit (The Kocaeli (Turkey) Earthquake of 17 August 1999). *Nat. Hazards*, **31**, 233–252.
- Şahoğlu, V., 2002. *Early Bronze Age Pottery from Liman Tepe and its Significance in the Archaeology of the Aegean*. PhD Thesis, Ankara University. (In Turkish), 427 p.
- Şahoğlu, V., 2005. Interregional Contacts Around the Aegean During The Early Bronze Age: New Evidence from the Izmir Region. *Anadolu Kardiyol. Derg.*, **27**, 97–120.
- Scott, D.B. and Medioli, F.S., 1986. Foraminifera as sea-level indicators. In: *Sea-Level Research: A Manual for the Collection and Evaluation of Data* (O. van de Plassche, ed.), pp. 435–456. Geo Books, Norwich.
- Scott, D.B., Medioli, F.S. and Schafer, C.T., 2001. *Monitoring in Coastal Environments Using Foraminifera and Thecamoebians*. Cambridge University Press, New York, 192 p.
- Stanley, D.J. and Warne, A.J., 1994. Worldwide Initiation of Holocene Marine Deltas by Deceleration of Sea-Level Rise. *Science*, **265**, 228–231.
- Wachsmann, S., 1998. *Seagoing Ships & Seamanship in the Bronze Age Levant*. Texas A&M University Press, College Station.
- Waterfield, R., 1998. *Herodotus. The Histories*. Herodotus: (translation; introduction and notes by C. Dewald), Oxford University Press, England, 840 p.

Received 21 November 2007; revised version accepted 08 December 2008